Voltage-dependent potassium channels in activated rat microglia

Wolfgang Nörenberg, Peter J. Gebicke-Haerter* and Peter Illes

*Department of Pharmacology, University of Freiburg, Hermann-Herder-Strasse 5 and *Department of Psychiatry, University of Freiburg, Hauptstrasse 5, D-79104 Freiburg, FRG*

1. Voltage-dependent currents of untreated (proliferating) and lipopolysaccharide (LPS)-treated rat microglial cells in culture were recorded using the whole-cell patch-clamp technique.

2. Membrane potentials showed prominent peaks at −35 mV and −70 mV. Membrane potentials of LPS-treated cells alternated between the two values. This may be due to a negative slope region of the *I–V* relation resulting in two zero current potentials.

3. From a holding potential of −70 mV, hyperpolarizing steps evoked an inwardly rectifying current both in proliferating and in LPS-treated cells, while depolarizing steps below −50 mV evoked an outwardly rectifying current only in LPS-treated microglia. The currents were K^+ selective, as indicated by their reversal potential of approximately 0 mV in symmetric K^+ concentrations (150 mM both intra- and extracellularly) and the reversal potential of the outward tail currents of approximately −90 mV at a normal extracellular K^+ concentration (4·5 mM).

4. The activation of the outward current could be fitted by Hodgkin–Huxley-type n^4 kinetics. The time constant of activation depended on voltage.

5. The inactivation of the inward and outward currents could be fitted by a single exponential. The time constant of the inward current inactivation was dependent on voltage, whereas the time constant of the outward current inactivation was virtually independent of voltage, except near the threshold of activation. Recovery of the outward from inactivation was slow and could be fitted by two exponentials. Responses to depolarizing steps were stable at 0·125 Hz, but greatly decreased from the first to the second pulse at 1 Hz.

6. The inactivation of the inward, but not of the outward, current disappeared in a low Na^+-containing medium (5 mM). The inward current was selectively inhibited by extracellular Cs^+ and Ba^{2+}. The outward current was selectively inhibited by Cd^{2+}, 4-aminopyridine and charybdotoxin. Replacement of intracellular K^+ by an equimolar concentration of Cs^+, and the extracellular application of tetraethylammonium and quinine inhibited both currents.

7. An increase of extracellular Ca^{2+} from 2 to 20 mM resulted in outwardly rectifying K^+ channels activating at more positive potentials. Omission of Ca^{2+} from the extracellular medium had the opposite effect. When the intracellular free Ca^{2+} was increased from 0·01 to 1 μM, the outward current amplitudes were depressed. The Ca^{2+} ionophore A23187 had a similar effect.

8. LPS-treated microglial cells possess inwardly and outwardly rectifying K^+ channels. The physiological and pharmacological characteristics of these two channel populations are markedly different. The inwardly rectifying channels exhibit only macrophage properties, while the outwardly rectifying channels exhibit mixed macrophage–lymphocyte properties.

Microglia are resident macrophages of the brain. Resting (ramified) microglia have a small cell body and several branching processes (Jordan & Thomas, 1988; Streit, Graeber & Kreutzberg, 1988; Thomas, 1992). Neuronal damage leads to a conversion of these cells to macrophages through at least one intermediate form called activated (reactive) microglia (Jordan & Thomas, 1988; Streit *et al.* 1988; Thomas, 1992). Activated cells have a round shape without processes, and are capable of both proliferation and phagocytosis (Rieske, Graeber, Tetzlaff, Czlonkowska, Streit & Kreutzberg, 1989). They can change into macrophage-like microglia, that present major histocompatibility antigens (MHC) types I and II, secrete cytokines (e.g. interleukin-1 and -6) and produce superoxide anions (Bignami, 1991; Dickson, Mattiace, Kure, Hutchins, Lyman & Brosnan, 1991). Such fully activated cells no longer proliferate but are still involved in phagocytosis. All these properties enable the microglia to participate in the first defence mechanism of the brain, which is often followed by invasion of blood-borne macrophages (Jordan & Thomas, 1988).

Although microglial cells have, at various times, been described as mesodermal or neuroectodermal in origin, evidence is emerging that assigns microglia to the monocyte–macrophage lineage. These cells enter the brain during early embryonic development and through a series of morphological transitions differentiate into microglia (Theele & Streit, 1993). Macrophages exhibit various voltage- or calcium-dependent ionic conductances, including voltage-dependent inactivating inward and outward potassium currents as well as calcium-dependent potassium currents (Gardner, 1990; Gallin, 1991). In contrast, the predominant potassium conductance in proliferating microglia is inwardly rectifying (Kettenmann, Hoppe, Gottmann, Banati & Kreutzberg, 1990; Banati, Hoppe, Gottmann, Kreutzberg & Kettenmann, 1991), although in a small percentage of these cells an outwardly rectifying potassium current has also been found (Korotzer & Cotman, 1992).

One of the compounds known to activate macrophages is bacterial lipopolysaccharide (LPS) (Adams & Hamilton, 1987; Hamilton & Adams, 1987). Human blood monocyte-derived macrophages only rarely exhibit an outwardly rectifying potassium conductance, but stimulation with LPS markedly increases the expression of this channel type (Nelson, Jow & Jow, 1992). Similarly, in rat microglia LPS-treatment leads to the expression of previously lacking outwardly rectifying potassium channels (Nörenberg, Gebicke-Haerter & Illes, 1992). The aim of the present study was to physiologically and pharmacologically characterize the LPS-induced current in microglia and to compare it with the inwardly rectifying potassium current also present in non-treated proliferating cells.

METHODS

Cell cultures

Mixed astroglial–microglial cell cultures were prepared from cerebral hemispheres of newborn Wistar rats as described previously (Keller, Jackisch, Seregi & Hertting, 1985). In brief, animals were killed by decapitation, meninges were removed, and forebrains were minced and gently dissociated by trituration in Hank's balanced salt solution. Cells were collected by centrifugation at 200 *g* for 10 min, resuspended in Dulbecco's modified Eagle's medium (DMEM), supplemented with 10 % fetal calf serum (FCS), plated onto 35 mm Falcon culture dishes (5×10^5 cells per dish), and incubated at 37 °C in a humidified atmosphere of 95 % air, 5 % CO_2. Media were prepared taking extreme care to avoid all potential sources of LPS contamination. Only those batches of FCS were used which had minimal LPS-content as tested by their ability to induce interleukin-1 production in cultured human blood monocytes (Northoff, Glück, Wölpl, Kubanek & Galanos, 1986). After 14 days of culture under LPS-free conditions, floating microglial cells were harvested and reseeded into 35 mm Petri dishes to give pure microglial cultures (Gebicke-Haerter, Bauer, Schobert & Northoff, 1989). Small cells (diameter, 5–8 μm) similar in appearance to ramified microglia with unipolar or bipolar processes were observed under phase contrast optics immediately after reseeding. When LPS (100 ng ml^{-1}) was added for 12–24 h, the microglial cells became circular in shape with ruffled edges (diameter, 15–23 μm) reminiscent of amoeboid microglia.

The identity of the cell types was previously confirmed both in mixed astrocyte and in isolated microglial cultures by immunocytochemical (Gebicke-Haerter *et al.* 1989) or enzyme-histochemical (Ganter, Northoff, Männel & Gebicke-Haerter, 1992) markers, such as ED1 (Dijkstra, Döpp, Joling & Kraal, 1985), nucleoside diphosphatase (NDPase), thiamin pyrophosphatase (TPPase) (Novikoff & Goldfischer, 1961) or lectin staining (Streit, 1990). Isolated microglial cultures were devoid of glial fibrillary acidic protein (GFAP)- and fibronectin-positive cells. Since all isolated cells were ED1-positive, it was concluded that only cells derived from the monocyte–macrophage lineage were present in those cultures. Microglial phagocytic behaviour was verified by incubation with latex beads and their responses to inflammatory stimuli were investigated. LPS, for example, enhanced synthesis of prostaglandin E_2 and stimulated production of interleukin-1 and -6 as well as synthesis of tumour necrosis factor (Gebicke-Haerter *et al.* 1989; Ganter *et al.* 1992).

Patch-clamp experiments

Membrane currents of proliferating and LPS-treated microglial cells were measured using the patch-clamp method in whole-cell (Hamill, Marty, Neher, Sakmann & Sigworth, 1981) or permeabilized-patch (Horn & Marty, 1988) configuration. The bath (extracellular) solution contained (mM): NaCl, 160; KCl, 4·5; $MgCl_2$, 1; $CaCl_2$, 2; *N*-2-hydroxyethylpiperazine-*N'*-2-ethanesulphonic acid (Hepes), 5; glucose 11; adjusted to pH 7·4 with NaOH. In experiments with 20 mM Ca^{2+} or 150 mM K^+, osmotic compensation was achieved by an equimolar decrease in Na^+. The low-Na^+ medium was prepared in the same way but contained 5 mM NaCl and 155 mM choline chloride. The Ca^{2+}-free medium was prepared by omitting Ca^{2+} and adding 1 mM ethylene glycol-bis-(β-aminoethylether)-*N,N,N',N'*-tetraacetic acid (EGTA). The pipette (internal) solution contained (mM): KCl, 150; $MgCl_2$, 2; $CaCl_2$, 1 (free Ca^{2+}, 0·01 μM); EGTA, 11; Hepes, 10; adjusted to pH 7·3 with KOH. The free Ca^{2+} concentration was increased to 1 μM by decreasing the concentration of EGTA to 1·1 mM and leaving the other components of the solution unchanged. In some experiments the intracellular KCl was replaced by CsCl and the pH was set to 7·3 by adding CsOH. Pipettes pulled from borosilicate capillaries (Vitrex BRI/E, Poly-Labo, Strasbourg, France) were coated with beeswax and dipped in Sigmacote

(Sigma, Deisenhofen, FRG) to minimize associated capacitive currents. The resistance of the electrodes was 2–5 MΩ. The seal resistance was 3–35 GΩ, and the input resistance of the cells ranged between 1–20 GΩ.

Compensation of capacitance (20–60 pF) and series resistance (6–25 MΩ) was achieved with the in-built circuitry of the patch amplifier (EPC-7, List Electronic, Darmstadt, FRG). Voltage-clamp protocols were generated with a stimulator (S-98, Medical Systems, Greenvale, NY, USA) or with a laboratory computer (ESCOM/486, Heppenheim, FRG). Data were digitized at 1–7 kHz (Model 1401, Cambridge Electronic Devices, Cambridge, UK) and then stored on and analysed with the computer. Experiments were carried out at room temperature (20–24 °C). In most experiments the leak current was negligible compared with the K^+ current; the data illustrated have not been corrected. Nevertheless, a leak current was subtracted before analysing K^+ conductances. Non-linear least-squares regression was used for fitting exponential Hodgkin–Huxley or Boltzmann functions to data.

After whole-cell configuration was achieved, the membrane potential was determined in the current-clamp mode. The system was left for 5–10 min to allow stabilization of the voltage dependency of various parameters. Unless stated otherwise, cells were held at −70 mV. With a few exceptions mentioned in the text, stimulation was 1 pulse $(8\ s)^{-1}$ (100–300 ms step duration) or 1 pulse $(30\ s)^{-1}$ (3 s step duration) to allow recovery from inactivation. When $I-V$ relations were determined, currents were usually elicited by both negative and positive voltage pulses of 300 ms duration given in steps of 20 mV from a holding potential of −70 mV.

Patches were permeabilized by nystatin (100 μM) contained in the normal internal medium of pipettes. An electrical continuity was established between the pipette and the cytoplasm of the cell 10–15 min after formation of a cell-attached patch.

All compounds except charybdotoxin were superfused at a flow rate of 2 ml min^{-1}. The maximum alterations of K^+ current amplitudes evoked by these compounds were evaluated after achieving a steady state (usually 4–8 min superfusion time). In the case of tetraethylammonium 10–15 min superfusion time was needed to reach a steady state. Similarly, cells were exposed to media with no Ca^{2+} or 20 mM Ca^{2+} for 10–15 min. Charybdotoxin was locally microperfused for 1 min by means of separate wide-bore pressurized (10 kPa) puffer pipettes, placed about 50 μm away from the cell under examination. Puffer application of drug-free extracellular solution had no effect ($n = 4$).

Materials

The following materials and drugs were used: Dulbecco's modified Eagle's medium, Hank's balanced salt solution, fetal calf serum (Gibco, Eggenstein, FRG); lipopolysaccharide from *Salmonella typhimurium* (Sebak, Aidenbach, FRG); nystatin, tetraethylammonium chloride, 4-aminopyridine, quinine hydrochloride, A23187 free acid (Sigma, Deisenhofen, FRG), charybdotoxin (Bachem, Bubendorf, Switzerland).

LPS was purified to homogeneity according to a method described by Galanos, Lüderitz & Westphal (1979) and supplied in aqueous solution of 1 mg ml^{-1}. It was further diluted in DMEM. Tetraethylammonium, 4-aminopyridine and quinine were dissolved in the bath medium. Stock solutions (1 mM) of charybdotoxin and A23187 were prepared with distilled water and dimethyl sulphoxide, respectively. Further dilutions were made in the bath medium. Stock solution (5 mM) of nystatin was prepared with dimethyl sulphoxide and dissolved further with pipette medium to give a final concentration of 100 μM.

Statistics

Where appropriate, means ± S.E.M. of n trials are shown. The Student's unpaired t test was used to compare means and Student's paired t test was used to compare means with zero. A probability level of 0·05 or less was considered to be statistically significant.

RESULTS

Activated microglia

Membrane potential

All microglial cells included in this part of the study were pretreated with LPS (100 ng ml^{-1}) for 12–24 h. Membrane potentials of 234 randomly chosen cells showed two prominent peaks, one at −35 mV and the other at −70 mV (Fig. 1*A*) with a mean value of −52·3 ± 1·1 mV. Although the membrane potential of more than half of the cell population was below −60 mV, the seal resistance was never less than 3 GΩ at a holding potential of −70 mV. Hence, there was no indication of poor recording conditions. When the membrane potential of six cells was recorded for a longer period of time, random fluctuations between two preferred values of around −35 and −70 mV were observed (Fig. 1*B*). In order to clarify the reason for these findings, cells were held at −90 mV and positive voltage steps of 300 ms duration were given in 5 mV increments up to −30 mV every 8 s (Fig. 1*C*). The steady-state currents measured in reponse to the voltage pulses were small; large inward or outward currents were evoked only by stepping below or above this potential range (see Fig. 2). The $I-V$ relation shown in Fig. 1*C* contains a region of negative slope conductance between −50 and −40 mV. The voltage axis was crossed at approximately −85 and −40 mV (note that because of a scatter within individual measurements, data points at −45, −40 and −35 mV are not significantly different from zero; $P > 0{\cdot}05$). This N-shaped $I-V$ relation may lead to two stable states of membrane potential. Fig. 1*D* displays the current response to the middle part of a voltage ramp from −140 to +40 mV (holding potential, −70 mV; ramp duration, 1 s; $n = 5$). This procedure yielded an $I-V$ curve similar to that obtained in response to individual voltage steps (compare Fig. 1*C* and *D*).

Voltage-dependent K^+ currents

In a subsequent series of experiments currents were elicited by both negative and positive voltage pulses given in steps of 20 mV from a holding potential of −70 mV; the pulse duration was 300 ms and the stimulation frequency 0·125 Hz (1 pulse every 8 s). With a few exceptions, this protocol was used throughout the paper to determine $I-V$ relations. Responses to voltage steps were similar, even when all cells were held at −70 mV, irrespective of their previous membrane potential. In a bath medium of normal $[K^+]$ (4·5 mM), hyperpolarizing steps beyond −70 mV produced inward currents (Fig. 2*A a* and *B*). For steps beyond

−130 mV, the current amplitudes decreased with time. Depolarizing steps elicited an outward current, which activated below −50 mV and exhibited a slight time dependence for voltage pulses below −10 mV (Fig. 2*A a*).

When *I–V* curves were determined in symmetric [K^+] (150 mM both in the bath medium and the pipette solution), a large resting inward current appeared at the holding potential (compare Fig. 2*A a* with *A b*). The peak currents increased in amplitude beyond −70 mV, became inward between −70 and 0 mV and reversed at around 0 mV (Fig. 2*A b* and *B*). Hence, the extrapolated reversal potential of the inward current was shifted to the right in the high-K^+ bath medium. In spite of equal [K^+] on both sides of the membrane, the *I–V* curve exhibited inward rectification. It is noteworthy that the time-dependent inactivation of the inward current almost disappeared in the high-K^+ bath medium; the time-dependent inactivation of the outward current greatly decreased, but still persisted (Fig. 2*A b*). In seven cells, the slope conductance of the inward current calculated between −110 and −130 mV (9·3 ± 2·0 nS) was increased in the high-K^+ bath medium (26·8 ± 4·1 nS; $P < 0·01$), while the slope conductance of the outward current calculated between +30 and +50 mV (8·9 ± 2·9 nS) was not changed (8·1 ± 3·5 nS; $P > 0·05$).

The reversal potential of the outward current was estimated from the reversal of the tail currents when [K^+] in the bath was 4·5 mM (Fig. 3). The cells were first stepped by a pre-pulse from −70 mV to a potential which activated the outward current (+30 mV) for 20 ms and then shifted back by a test pulse to various potentials between −100 and −40 mV in 10 mV steps for 300 ms (Fig. 3*A*). Since below −70 mV the activation of the inwardly rectifying current interferes with reliable measurements, Cs^+ (1 mM) was added to the bath to block inward currents. The amplitude of the tail current (measured 10 ms after the beginning of the test pulse minus steady-state current) was plotted *versus* the voltage of the test pulse. This procedure (Gallin & Sheehy, 1985) underestimates the actual tail current amplitudes, but can be used to determine the reversal potential of the current. On the other hand, a possible distortion of the early current

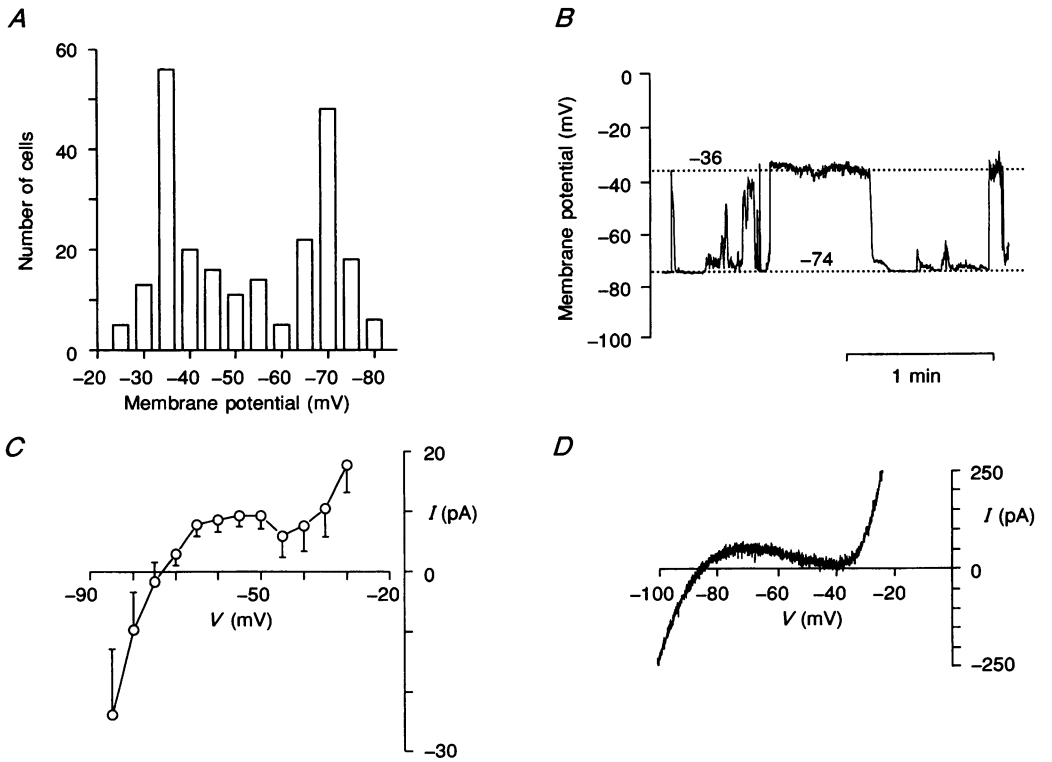

Figure 1. Membrane potential of lipopolysaccharide (LPS)-treated rat microglia
A, the membrane potential was measured under whole-cell patch conditions immediately after gaining access to the cell interior. It had a distribution showing two prominent peaks around −35 and −70 mV in 234 cells. *B*, random fluctuations between various membrane potential states with the preferred values of −36 and −74 mV in a microglial cell. Recording started 5 min after achieving whole-cell configuration. *C*, *I–V* relations of cells held at −90 mV. Depolarizing voltage steps (300 ms duration) were applied every 8 s in 5 mV increments up to −30 mV. Current amplitudes were measured in the middle of the voltage steps, i.e. under steady-state conditions. The resulting *I–V* curve shows N-shaped behaviour. Means ± S.E.M. from 5 cells. *D*, membrane response of a microglial cell to the middle part of a voltage ramp (−70 mV holding potential, 1 s duration, from −140 to +40 mV).

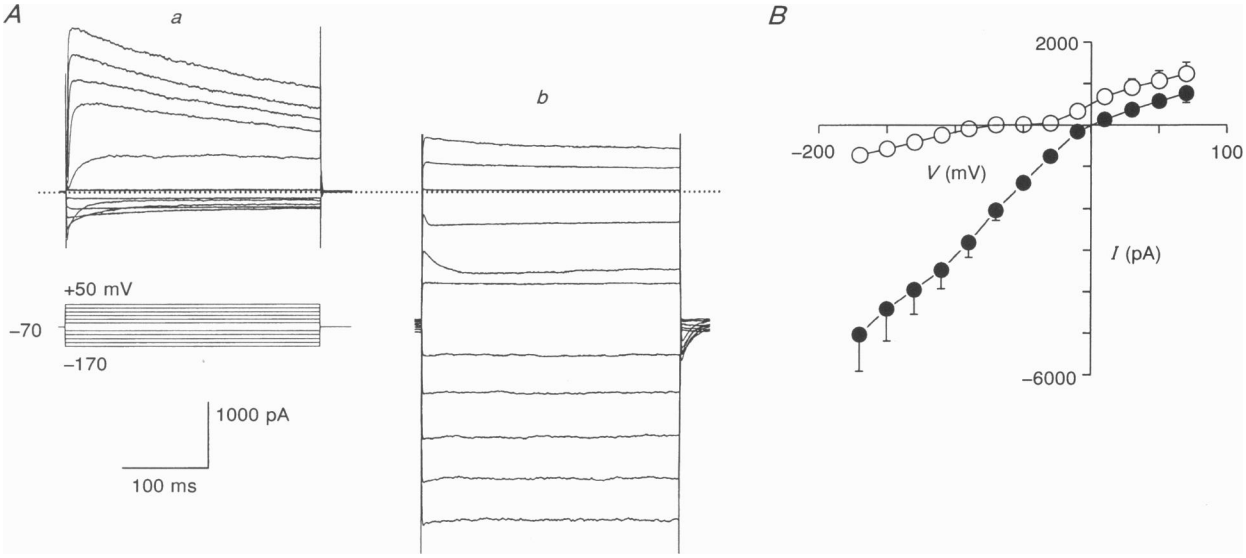

Figure 2. Dependence of voltage-sensitive conductances of LPS-treated rat microglia on the extracellular K^+ concentration

Aa, currents recorded in normal K^+ (4·5 mM) bath solution (upper panel). Voltage pulses (lower panel) were applied every 8 s from a holding potential of −70 mV in 20 mV increments. Step range was from −170 to +50 mV. *Ab*, currents of the same cell recorded in elevated K^+ (150 mM) bath medium. Under these conditions K^+ concentrations are symmetric in the extra- and intracellular space. The dotted line indicates the zero current level. *B*, peak *I–V* relations of 5 cells in 4·5 (○) and 150 mM (●) extracellular K^+. Same protocol as in *A*, except that the effect of an additional depolarizing step to +70 mV is also shown. Means ± S.E.M. from 5 cells.

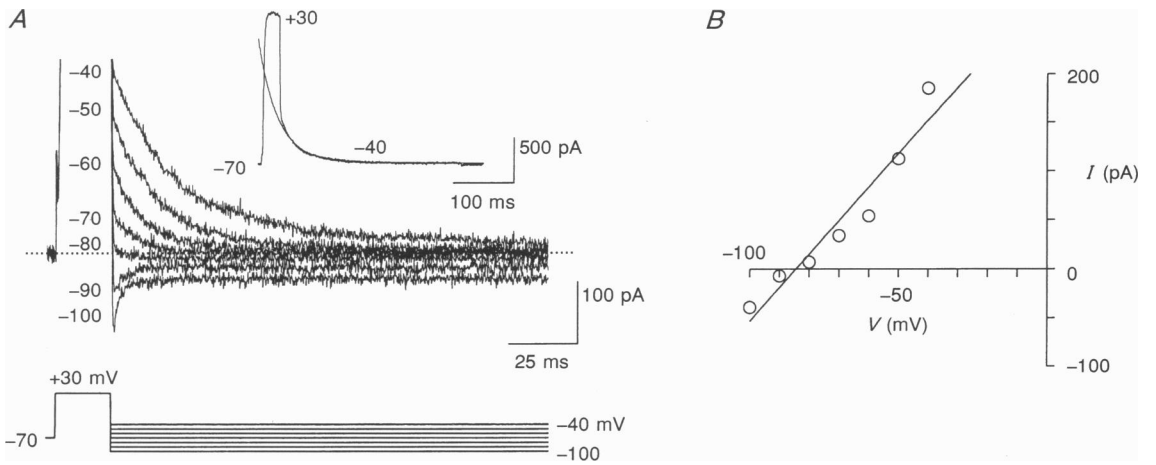

Figure 3. Reversal potential of the outward current in LPS-treated rat microglia

A, tail currents (upper panel) evoked by a double-pulse protocol (lower panel). The cell was held at −70 mV and stepped by a 20 ms pre-pulse to +30 mV (only partially shown; compare with inset). Then, the membrane was repolarized by 300 ms test pulses to the levels indicated. This procedure was repeated every 8 s. Cs^+ (1 mM) was present in the bath medium to avoid contamination of tail currents by the inward conductance. The time constant of tail current inactivation (τ) was assessed by fitting a single exponential to the traces, starting 10 ms after onset of the test pulse (see inset). *B*, *I–V* relation for tail currents (measured 10 ms after onset of the test pulse minus steady-state current) from the cell shown in *A*. The reversal potential (−84 mV) was determined by fitting a least-squares linear regression (continuous line) to the data.

phase by the capacitive artifact is avoided. In the example shown in Fig. 3*B*, the resulting *I–V* curve reversed at a potential of −84 mV; in seven experiments this value was −90·5 ± 1·7 mV, which is close to the calculated potassium equilibrium potential ($E_K = -89$ mV). The reversal potential of the tail currents before the application of Cs^+ was −84·7 ± 2·1 mV ($n = 7$), which is lower than the calculated K^+ equilibrium potential. This result underlines the need to take measurements in the presence of Cs^+ (1 mM). The decay of the tail current obtained in a Cs^+-containing medium (1 mM) and 10 ms after the beginning of the test pulse, was fitted with a single exponential (Fig. 3*A*, inset). The time constant was 33·7 ± 2·3 ms at −40 mV and gradually declined with increasing membrane potentials to 9·8 ± 1·3 ms at −70 mV ($n = 7$).

Chord conductance

The chord conductance of the inward current was calculated from *I–V* curves determined by stepwise hyperpolarizations from a holding potential of 0 mV (where the outward current is largely inactivated; see Fig. 7), but otherwise with the usual protocol. Leak conductance, measured for steps to −10 and −20 mV, was subtracted. A potassium equilibrium potential of −89 mV was used for calculation. The relation of conductance to voltage of six cells is presented in Fig. 4*A*. The K^+ conductance values of each cell (G_K) were normalized to 1·0 by their maximum ($G_{K,max}$) so they could be pooled. The voltage at which the maximum conductance was observed varied between −100 and −150 mV (at −110 mV it was 10·5 ± 1·7 nS; $n = 6$); consequently the pooled conductances

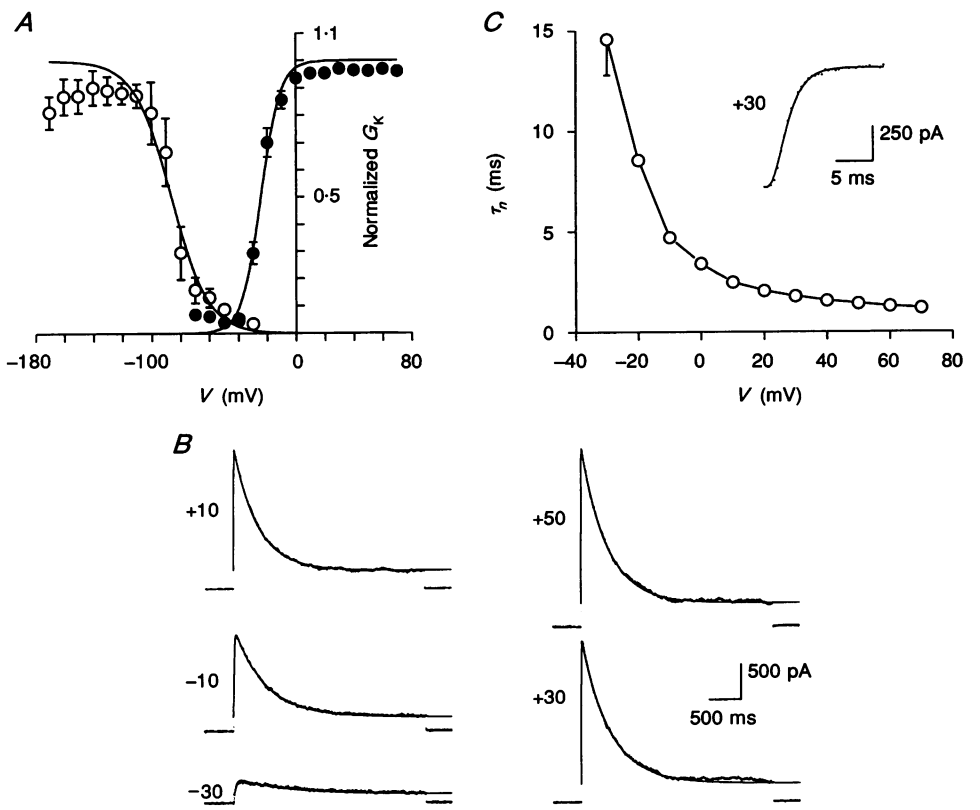

Figure 4. Activation of voltage-dependent K^+ conductances in LPS-treated rat microglia
A, chord conductance–voltage relation. The conductance was calculated by transforming peak currents using the equation $G_K = I/V - V_K$ where I is the peak amplitude at a given potential (V) and V_K equals the assumed K^+ reversal potential ($E_K = -89$ mV). G_K of each cell was normalized to 1·0 by its maximum $G_{K,max}$. Currents were elicited by 300 ms voltage steps applied every 8 s to the potentials indicated. The holding potential was 0 mV for the inward conductance (○; $n = 6$). Leak conductance, measured for steps to −10 and −20 mV, was subtracted. The holding potential was −70 mV for the outward conductance (●; $n = 12$). Continuous curves represent best fits to a Boltzmann distribution according to eqn (1). Note that around −45 mV, membrane conductances are virtually zero (see also Fig. 1). *B*, outward currents elicited by 3 s voltage steps applied every 30 s to the potentials indicated. The holding potential was −70 mV. Continuous curves represent best fits to a Hodgkin–Huxley-type n^4j model according to eqn (2). *C*, activation time constants (τ_n) as function of voltage. Values of τ_n were obtained by fitting Hodgkin–Huxley kinetics of the form $I_{total} = I_{K,max}(1 - e^{-t/\tau_n})^4$ to the rising phase of outward current amplitudes (see inset). Stimulation was with 300 ms voltage steps applied every 8 s in the range −30 to +70 mV in 10 mV increments. The holding potential was −70 mV. Means ± S.E.M. from 7 cells.

were less than 1·0 at all potentials. The continuous line through the data points represents the best fit of the peak conductance to a Boltzmann distribution of the form:

$$G_K/G_{K,max} = 1/\{1 + \exp[(V - V_k)/k]\}, \quad (1)$$

where k is a constant (−12·4 ± 2·2 mV; $n = 6$) characterizing the steepness of the voltage dependence, and V_k (−86·1 ± 2·5 mV; $n = 6$) represents a constant that locates the curve along the voltage axis. The conductance is half-maximal when the membrane potential (V) equals V_k. The data were fitted by non-linear least-squares regression. Apparently, the conductance is activated at rest (16 % at the preferred value of −70 mV) and thus contributes to the resting membrane potential of the cell.

The chord conductance of the outward current was calculated from another twelve experiments (at +30 mV it was 10·2 ± 1·8 nS; $n = 12$). In these cells the I–V curves were determined by stepwise depolarizations from a holding potential of −70 mV. The relation of normalized conductance to voltage is presented in Fig. 4*A*. The conductance activated positive to −40 mV and plateaued around 0 mV. The continuous line drawn through the points was traced by a similar procedure to that in Fig. 4*A*. The constant k was 6·7 ± 0·8 mV ($n = 12$) and V_k was −24·4 ± 0·9 mV ($n = 12$).

Kinetics of activation

Figure 4*B* shows curves drawn through the data points of the outward current by using a Hodgkin–Huxley-type (1952) n^4j model given by the equation:

$$I_{total} = I_{K,max}(1 - e^{-t/\tau_n})^4 e^{-t/\tau_j} + I_l, \quad (2)$$

where I_{total} is the total current, $I_{K,max}$ is the maximum current available at a given potential, I_l is the time-independent leak current, and τ_n and τ_j are the time constants of activation and inactivation, respectively. This model provides a good description of current amplitudes evoked by 3 s voltage steps to various potentials. A power of 4 gave the best over-all fit. The activation time constant (τ_n) was determined by fitting n^4 kinetics to the sigmoidal rising phase of current amplitudes evoked by shorter pulses (300 ms). τ_n was 14·6 ± 1·8 ms ($n = 7$) at −30 mV and decreased to 2·5 ± 0·1 ms ($n = 7$) at +10 mV (Fig. 4*C*). It did not change considerably at membrane potentials beyond +10 mV and was 1·8 ± 0·1 ms at +30 mV ($n = 7$).

The inward current activated with a much faster time course than the outward current. Hence, the capacitive transients interfered with the reliable determination of the time constants ($n = 7$).

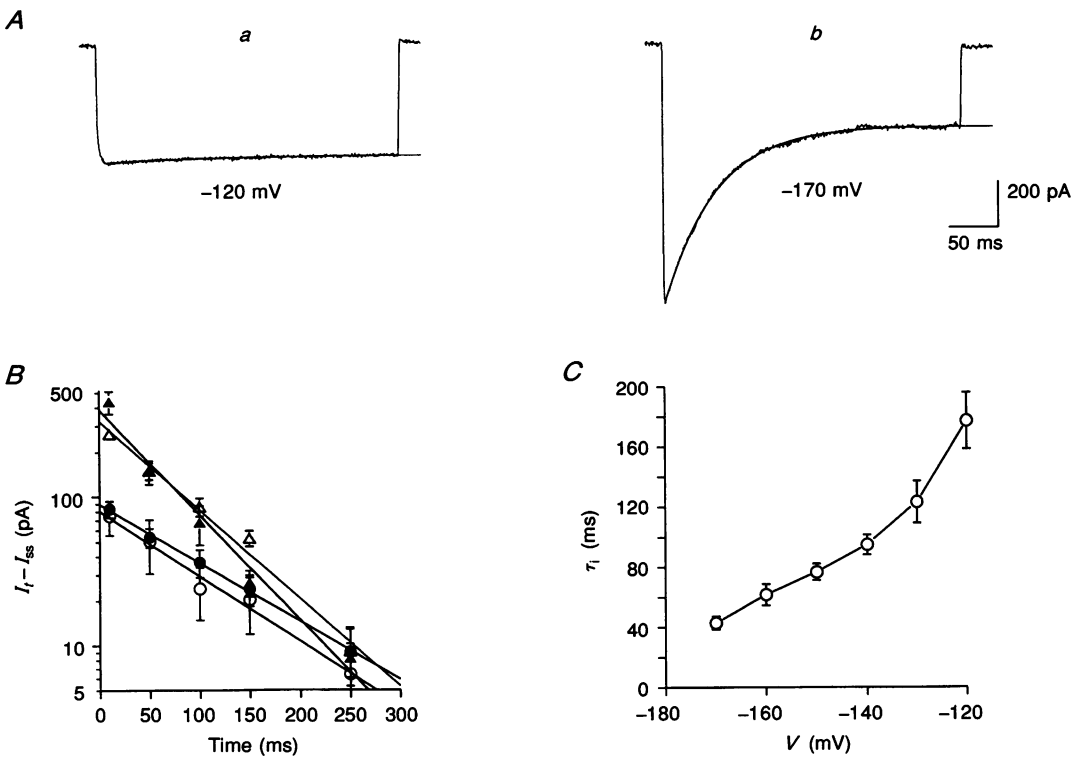

Figure 5. Inactivation of the inward K^+ current in LPS-treated rat microglia
A, current responses to 300 ms hyperpolarizing voltage steps from a holding potential of −70 mV to −120 (*Aa*) and −170 mV (*Ab*), respectively. The time constant of inactivation (τ_l) was assessed by fitting a single exponential to the traces. *B*, plot of inactivating inward currents as a function of time. Mean amplitudes were expressed as current (I_t) measured at various times after onset of the test pulse minus steady-state current (I_{ss}). Currents were evoked by 300 ms voltage steps from a holding potential of −70 mV to −120 (○), −130 (●), −150 (△) and −170 mV (▲). *C*, plot of inactivation time constant (τ_l) as a function of voltage. Means ± S.E.M. from the same 7 cells as shown in *B*.

Kinetics of inactivation

Inward currents declined during 300 ms hyperpolarizing pulses (Fig. 5). This decline was satisfactorily approximated by a single exponential function for voltage steps to both −120 and −170 mV from a holding potential of −70 mV (Fig. 5*Aa* and *b*). The current amplitudes determined at each period of time (I_t) were subtracted from the steady-state current determined at the end of the pulse (I_{ss}) and were plotted *versus* time (Fig. 5*B*). This plot confirmed that steps to potentials between −120 and −170 mV produced currents with an exponential decline during sustained membrane hyperpolarization. The time constant of decay was 177·3 ± 18·7 ms at −120 mV and decreased with increasing hyperpolarization to 42·8 ± 4·5 ms at −170 mV ($n = 7$; Fig. 5*C*).

Outward currents also exponentially declined during depolarizing pulses, albeit with a slower time course than the inward currents (Fig. 6). Pulses of 3 s duration were used to evoke outward currents. The time constant of decay was 2·5 ± 0·9 s at −30 mV; positive to this potential it was consistently smaller and did not show any voltage dependence (433·2 ± 13·7 ms at +30 mV; $n = 5$) (Fig. 6*C*).

The voltage dependence of steady-state inactivation of the outward current was studied by varying the holding potential between −100 and +10 mV and determining the peak currents during depolarizing test pulses to +30 mV (Fig. 7*A*). The normalized peak currents are fitted in Fig. 7*B* by a Boltzmann function identical with eqn (1). The constant k was −7·9 ± 0·8 mV ($n = 6$) and V_k was −48·3 ± 0·9 mV ($n = 6$).

Figure 8 shows outward currents evoked by thirteen repetitive pulses from −70 mV to +30 mV (300 ms duration). Recording was in the whole-cell or nystatin-permeabilized patch configuration. At a frequency of 0·125 Hz (interpulse interval, 8 s) the responses did not decrease significantly from the first to the second current amplitude (whole-cell: 7·4 ± 2·6 %, $n = 4$, $P > 0·05$; nystatin: 12·7 ± 4·9 %, $n = 4$, $P > 0·05$; Fig. 8*A*). In contrast, at a frequency of 1 Hz (interpulse interval, 1 s) the responses markedly declined from the first to the second current amplitude (whole-cell: 57·8 ± 3·5 %, $n = 4$, $P < 0·01$; nystatin: 60·7 ± 8·5 %, $n = 4$, $P < 0·01$; Fig. 8*B*). There was no further decline of the current amplitudes during the train at 0·125 Hz either in the whole-cell (13th amplitude: 15·0 ± 8·5 %, $n = 4$, $P > 0·05$ when compared with the 2nd amplitude) or the nystatin-permeabilized patch configuration (13th amplitude: 19·8 ± 7·1 %; $n = 4$; $P > 0·05$ when compared with the 2nd amplitude). However, in the whole-cell configuration, but not in the nystatin-permeabilized patch configuration,

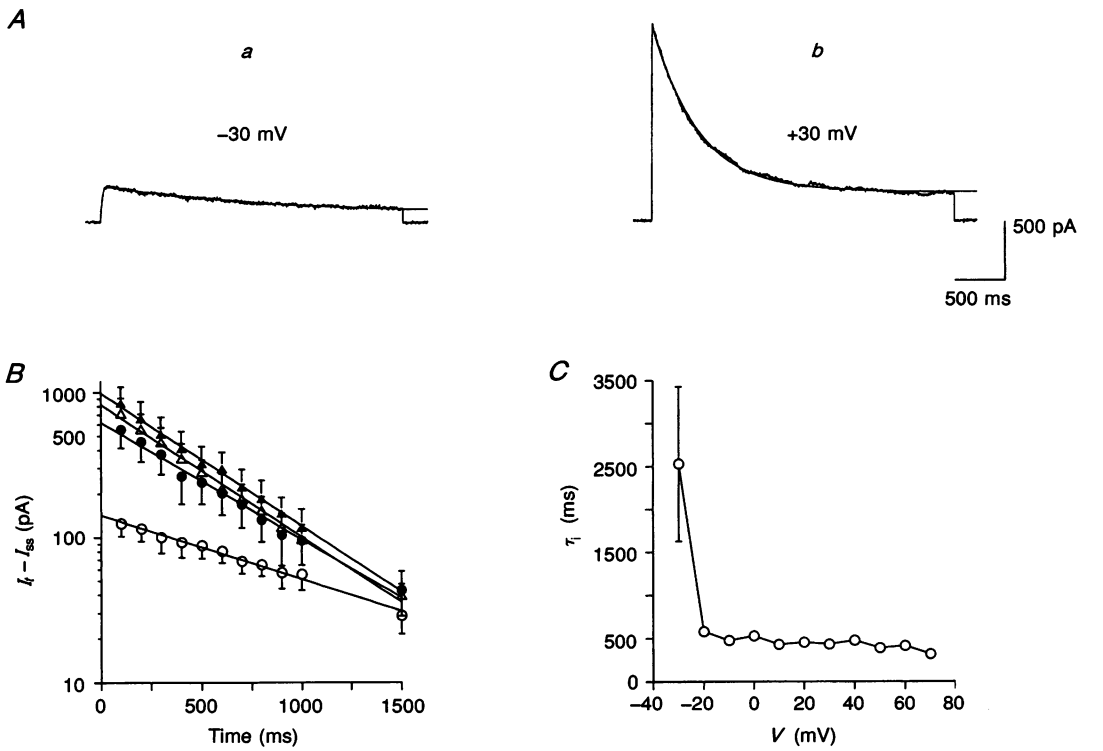

Figure 6. Inactivation of the outward K^+ current in LPS-treated rat microglia
A, current responses to 3 s voltage steps from a holding potential of −70 mV to −30 (*Aa*) and +30 mV (*Ab*), respectively. The time constant of inactivation (τ_i) was assessed by fitting a single exponential to the traces. *B*, plot of inactivating inward currents as a function of time. Mean amplitudes were expressed as current (I_t) measured at various times after onset of the test pulse minus steady-state current (I_{ss}). Currents were evoked by 3 s voltage steps from a holding potential of −70 mV to −30 (○), −10 (●), +10 (△) and +30 mV (▲). *C*, plot of inactivation time constant (τ_i) as a function of voltage. Means ± S.E.M. from the same 5 cells as shown in *B*.

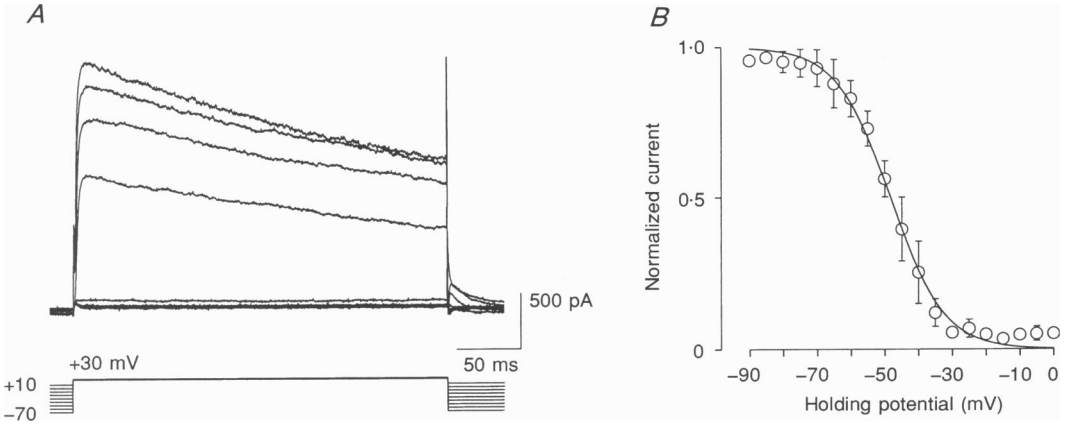

Figure 7. Voltage dependence of steady-state inactivation of the outward current in LPS-treated rat microglia
A, current amplitudes (upper panel) evoked from various holding potentials by 300 ms test pulses to +30 mV (lower panel). Illustrated are currents from a cell whose holding potential was changed between −70 and +10 mV in 10 mV increments. Individual holding potential levels were maintained for 2 min prior to the application of test pulses in order to reach equilibrium conditions. *B*, normalized peak currents from 6 cells plotted *versus* the holding potential. 300 ms test pulses were applied to +30 mV from a holding potential which ranged from −90 to 0 mV. Continuous curves represent best fits to a Boltzmann distribution similar to eqn (1).

current amplitudes continued to decline slightly with increasing number of pulses at 1 Hz. The thirteenth current amplitude decreased by 72·9 ± 3·6 % ($n = 4$, $P < 0{\cdot}01$ when compared with the 2nd current) in the whole-cell, and by 64·0 ± 6·3 % ($n = 4$, $P > 0{\cdot}05$ when compared with the 2nd current) in the nystatin-permeabilized patch configuration. This suggests that soluble intracellular factors lost during whole-cell recording have no major function in regulating the outward current.

Recovery from inactivation of the outward current

In subsequent experiments pairs of identical depolarizing voltage steps to +30 mV for 300 ms were applied separated by a variable interval at the holding potential of −70 mV (Fig. 9*A*). The ratio of the peak current during the second pulse to that during the first pulse (I_2/I_1) is a measure of the degree of recovery during the interval between the two pulses. The inactivated fraction of the peak amplitude was expressed by $1 - I_2/I_1$, and the logarithm of this value was plotted against the interval in Fig. 9*B*. The results show that recovery is fitted by the sum of two exponentials, with time constants of 2·2 ± 0·5 s and 16·1 ± 4·0 s ($n = 5$ for both). There was an early fast recovery with a similar time constant as that of the inactivation; afterwards the recovery was slower.

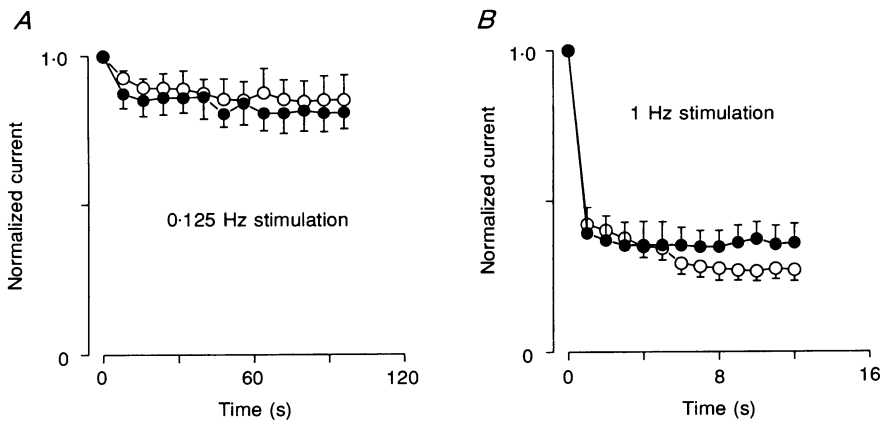

Figure 8. Frequency dependence of inactivation of the outward current in LPS-treated rat microglia
Thirteen repetitive pulses (300 ms duration) were applied from a holding potential of −70 mV to +30 mV at frequencies of 0·125 (*A*) or 1 Hz (*B*). Recording was in the whole-cell (○) or nystatin-permeabilized patch (●) configuration. Peak currents were normalized with respect to the first amplitude in the train. Means ± S.E.M. from 4 cells both in *A* and *B*.

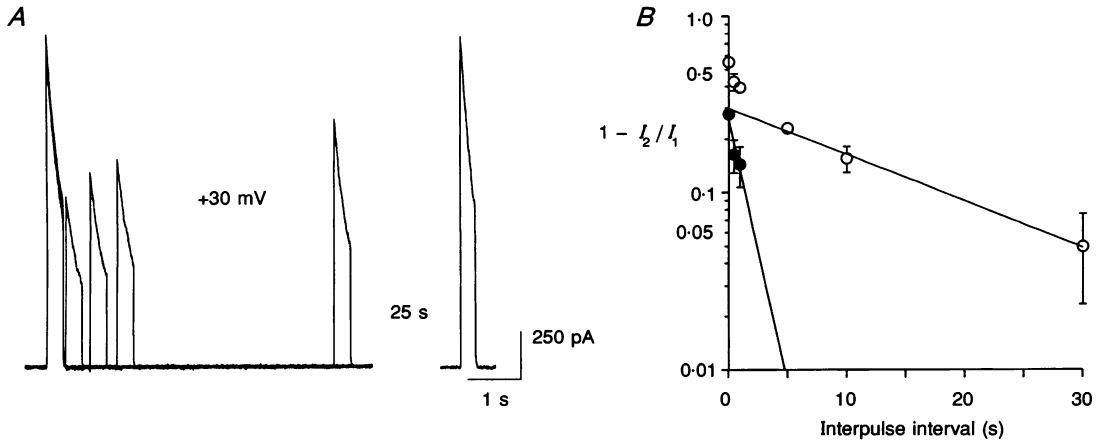

Figure 9. Time course of recovery from inactivation of the outward current in LPS-treated microglia

A, currents evoked by identical pairs of pulses (300 ms, from a holding potential of −70 mV to +30 mV). Pulses were separated by intervals of 0·05, 0·5, 1, 5 and 30 s. Between two double-pulses 1 min was allowed for complete recovery. *B*, inactivated fraction of the peak amplitude $(1 - I_2/I_1)$ plotted on a semilogarithmic scale against the duration of the interpulse interval. The sum of two single exponentials was needed to fit the time course of recovery thereby revealing a slow (○) and a fast component (●). Means ± S.E.M. from 5 cells.

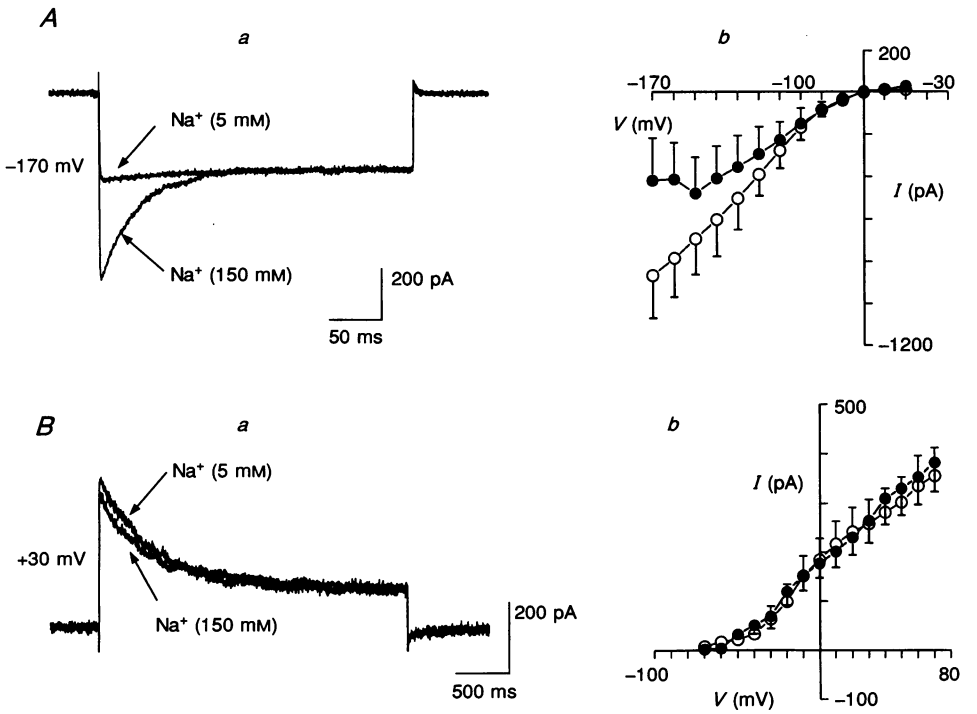

Figure 10. Effect of extracellular Na^+ on current inactivation in LPS-treated rat microglia

Aa, inward currents evoked by 300 ms voltage steps from a holding potential of −70 mV to −170 mV in normal (150 mM) Na^+-containing bath medium and after replacement of all but 5 mM Na^+ by choline. *Ab*, *I–V* relations obtained in 150 (○) and 5 mM (●) extracellular Na^+. Currents were evoked by 300 ms voltage pulses every 8 s from a holding potential of −70 mV. Pulse range was from −170 to −50 mV in 10 mV increments. Means ± S.E.M. from 5 cells. *Ba*, outward currents evoked by 3 s voltage steps from a holding potential of −70 mV to +30 mV in normal (150 mM) Na^+-containing bath medium and after replacement of all but 5 mM Na^+ by choline (same cell as in *Aa*). *Bb*, *I–V* relations obtained in 150 (○) and 5 mM (●) extracellular Na^+. Currents were evoked by 3 s voltage pulses every 30 s from a holding potential of −70 mV. Pulse range was from −60 to +70 mV in 10 mV increments. Means ± S.E.M. from the same 5 cells as shown in *Ab*.

Na^+ dependence of activation

In the following experiments $I-V$ curves were determined by the usual procedure from a holding potential of −70 mV. A reduction of the Na^+ concentration in the bath from 150 to 5 mM decreased the amplitude of the inward current (e.g. evoked by a pulse to −170 mV; Fig. 10*Aa*) and abolished its time-dependent inactivation. In contrast, both the outward current amplitude (e.g. evoked by a pulse to +30 mV; Fig. 10*Ba*) and its inactivation time course was unchanged in a low-Na^+ bath medium. This ionic manipulation resulted in a shallower $I-V$ relation of the inward current, and a negative slope region below −150 mV, without any change in the equilibrium potential (Fig. 10*Ab*). The $I-V$ curve of the outward current did not change in a low-Na^+ bath medium (Fig. 10*Ba*).

Effects of cations and pharmacological blockers of K^+ channels

The inward current was blocked both by extracellular Cs^+ (1 mM) and Ba^{2+} (5 mM), while the outward current was not influenced by these ions (Fig. 11*A*; Table 1). When K^+ was substituted in the pipette solution with an equimolar concentration of Cs^+ (150 mM), the outward conductance was blocked over the whole range of depolarizing steps, but the inward conductance was inhibited only at strongly hyperpolarized potentials (Fig. 11*B*). In addition, a resting inward conductance occurred at the holding potential and inward currents inactivated fast with Cs^+-containing pipette solutions (Fig. 11*Ba*). There was no indication of the existence of voltage-dependent Na^+ or Ca^{2+} currents under these conditions.

4-Aminopyridine (1 mM) and the higher concentration (100 nM) of charybdotoxin almost abolished the outward current (Table 1). The lower concentration (10 nM) of charybdotoxin depressed the outward current by only 40 % (Table 1). Quinine (1 mM) and tetraethylammonium (10–20 mM) blocked both the inward and the outward currents (Table 1). Quinine (1 mM) was more potent in inhibiting the outward than the inward conductance, while tetraethylammonium (10–20 mM) had a concentration-dependent but similar effect on the two currents. Cd^{2+} did not affect the inward, but depressed the outward, conductance (Table 1).

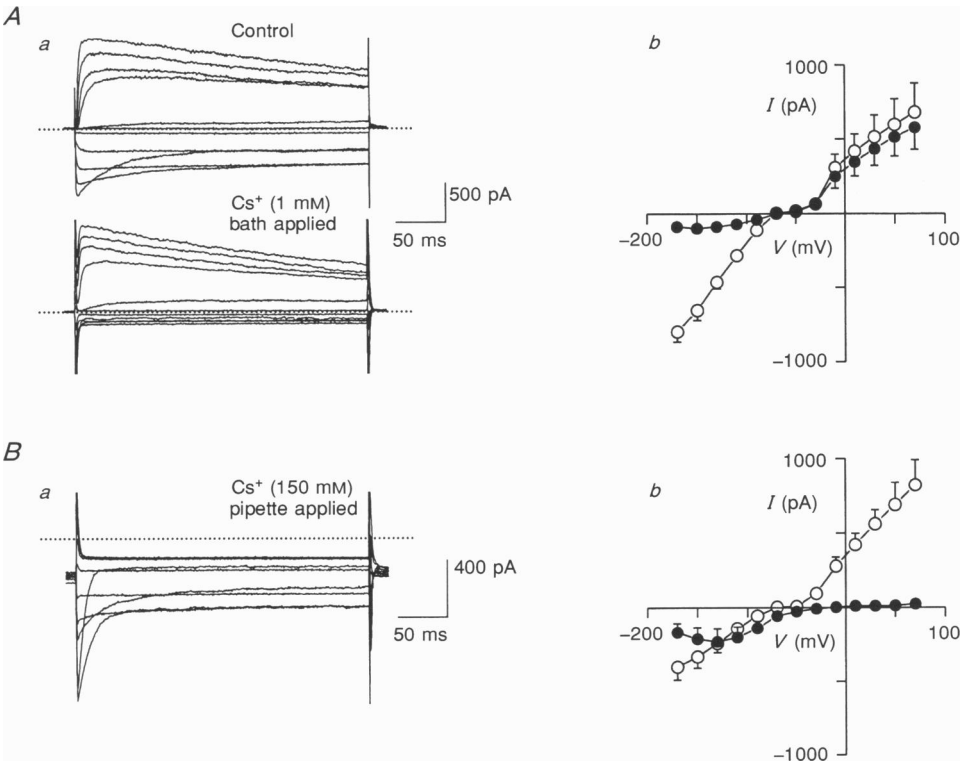

Figure 11. Effect of Cs^+ on the outward current in LPS-treated rat microglia
Aa, two families of current amplitudes elicited in the same cell before and after addition of Cs^+ (1 mM) to the bath medium. Currents were evoked by 300 ms voltage pulses every 8 s from a holding potential of −70 mV. Pulse range was from −170 to +50 mV in 20 mV increments. The dotted lines indicate the zero current level both in *Aa* and *Ba*. *Ab*, $I-V$ relations obtained before (○) and after (●) superfusion with a bath solution containing Cs^+ (1 mM). Same voltage protocol as in *Aa*. Means ± S.E.M. from 5 cells. *Ba*, family of current amplitudes elicited in a cell internally microdialysed with a pipette solution containing Cs^+ (150 mM). *Bb*, $I-V$ relations of two groups of cells from which recording was with a pipette solution containing K^+ (150 mM;○) or Cs^+ (150 mM; ●) as the main cation. Means ± S.E.M. from 5 cells each. The voltage protocols in *Ba* and *Bb* were similar to that in *Aa*.

Effect of changes in the Ca^{2+} concentration

Variations of the extracellular Ca^{2+} concentration between 0 and 20 mM had no major effect on the amplitude of the outward current (Fig. 12*A*). In these series of experiments 10 mV steps were made from a holding potential of −70 mV. The *I–V* curve in Fig. 12*A* shows only current amplitudes evoked by 20 mV steps. However, in the inset to this figure current amplitudes evoked by 10 mV steps are plotted on a larger voltage scale. This demonstrates more clearly that the omission of Ca^{2+} from the bath medium results in K^+ channels activating at more negative potentials. An increase in extracellular [Ca^{2+}] from 2 to 20 mM has the opposite effect on K^+ channel activation. In contrast to the outward current, the inward current was depressed in a high-Ca^{2+} (20 mM) medium (39·9 ± 10·9 %, $n = 5$, $P < 0·05$) at steps from −70 to −170 mV.

The standard pipette solution contains 0·01 μM free Ca^{2+}. When the internal free-Ca^{2+} concentration was increased to 1 μM, the outward, but not the inward, current decreased (Fig. 12*B*). Recordings with 0·01 and 1 μM internal Ca^{2+} were carried out alternately on cells from the same culture dishes. In the following experiments, the concentration of internal Ca^{2+} was increased by incubating microglial cells with the ionophore A23187 (1 μM). A significant decrease of the outward current amplitude evoked by a step from −70 to +30 mV (32·8 ± 3·7 %, $n = 6$, $P < 0·01$) was evident in the presence of the ionophore. When the same experiment was repeated in a Ca^{2+}-free bath medium, A23187 (1 μM) had no effect (−2·5 ± 12·7 % inhibition, $n = 6$, $P > 0·05$).

Proliferating microglia

Membrane potential

The membrane potential of eighty-one microglial cells measured 12–24 h after plating, had a similar distribution to that of microglia pretreated for 12–24 h with LPS (100 ng ml^{-1}). There were two prominent peaks at −35 and −70 mV in both groups and the mean values were also similar (proliferating: −50·0 ± 1·7 mV, $n = 81$; LPS-treated: −52·3 ± 1·1 mV, $n = 234$, $P > 0·05$).

Voltage-dependent K^+ current

Currents were elicited by both negative and positive voltage pulses given in steps of 20 mV from a holding potential of −70 mV. The pulse duration was 100 ms and the stimulation frequency was 0·125 Hz (1 pulse every 8 s). In contrast to LPS-treated microglia, only hyperpolarization-evoked inward currents were observed in eighty-one proliferating cells; depolarizing steps were without effect (compare Figs 2 and 13). However, in six additional cells a depolarization-evoked outward current was also present. Hence, in approximately 7 % of the proliferating cell population the pattern of current responses was similar to that in LPS-treated microglia.

Inward currents were produced by hyperpolarizing steps beyond −70 mV. For steps beyond −130 mV, the current amplitudes decreased with time (Fig. 13*A*). There was no time-dependent decline of the inward current when the external Na^+ was lowered from 160 to 5 mM ($n = 4$; not shown). The inward conductance was blocked by extracellular

Table 1. Effects of potassium channel blockers and Cd^{2+} on the amplitude of voltage-sensitive inward and outward potassium currents in LPS-activated rat microglia

Treatment	Concentration	Number of experiments	Inhibition of inward current (%)	Inhibition of outward current (%)
Cs^+	1 mM	5	88·5 ± 4·3**	12·7 ± 4·6
Ba^{2+}	5 mM	6	85·8 ± 6·5**	13·6 ± 10·5
Cd^{2+}	1 mM	7	0·8 ± 4·1	57·0 ± 2·4**
4-Aminopyridine	1 mM	5	0·2 ± 4·6	89·7 ± 2·0**
Quinine	1 mM	5	43·1 ± 7·6*	96·3 ± 1·2**
Charybdotoxin	10 nM		13·4 ± 7·7	42·5 ± 6·5**
	100 nM	6	13·9 ± 5·8	80·3 ± 4·2**
Tetraethyl-ammonium	10 mM	5	58·8 ± 13·5*	42·6 ± 4·6**
	20 mM	5	73·5 ± 9·2**	54·9 ± 4·6**

Cultured microglial cells were pretreated for 12–24 h with LPS (100 ng ml^{-1}). Currents were elicited from a holding potential of −70 mV by both negative and positive voltage pulses of 300 ms duration given in steps of 20 mV. Stimulation was every 8 s. After determining an *I–V* relation, all compounds and ions were added for 4–8 min to the bath. Exceptions were tetraethylammonium which was bath applied for 10–15 min and charybdotoxin which was pressure ejected from micropipettes for 1 min. Then a new *I–V* relation was determined in the presence of these compounds. Only two current amplitudes were chosen for further evaluation, namely the inward current evoked by a step to −170 mV, and the outward current evoked by a step to +30 mV. The percentage inhibition of these amplitudes by the compounds and ions tested was calculated. Statistically significant differences are indicated: *$P < 0·05$; **$P < 0·01$.

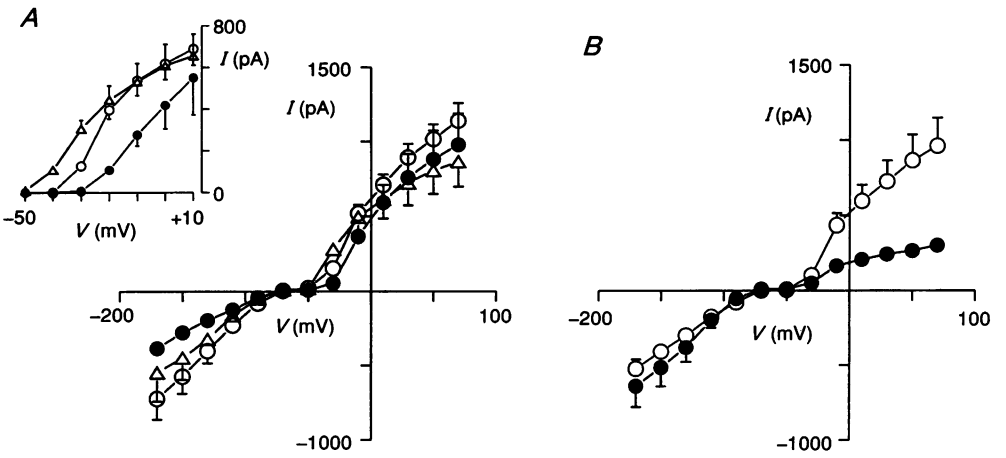

Figure 12. Effects of Ca^{2+} on the outward current in LPS-treated rat microglia
A, $I-V$ relations of cells perfused with a bath medium containing normal [Ca^{2+}] (2 mM; ○; $n = 11$), and subsequently with a bath medium containing [Ca^{2+}] (20 mM; ●; $n = 5$) or no Ca^{2+} and EGTA (1 mM; △; $n = 6$). Currents were evoked by 300 ms voltage pulses every 8 s from a holding potential of −70 mV. Pulse range was from −170 to +70 mV in 10 mV increments. Means ± S.E.M. from n cells. Results obtained in normal Ca^{2+}-containing (2 mM) bath medium were pooled. Inset, data replotted from *A* on a larger voltage scale. *B*, $I-V$ relations of two groups of cells from which recording was with a pipette solution containing Ca^{2+} (1 mM) and EGTA (11 mM) (intracellular free Ca^{2+}; 0·01 μM; ○) or with a pipette solution containing Ca^{2+} (1 mM) and EGTA (1·1 mM) (intracellular free Ca^{2+}; 1 μM; ●). Means ± S.E.M. from 5 cells each. The voltage protocol in *B* was similar to that in *A*.

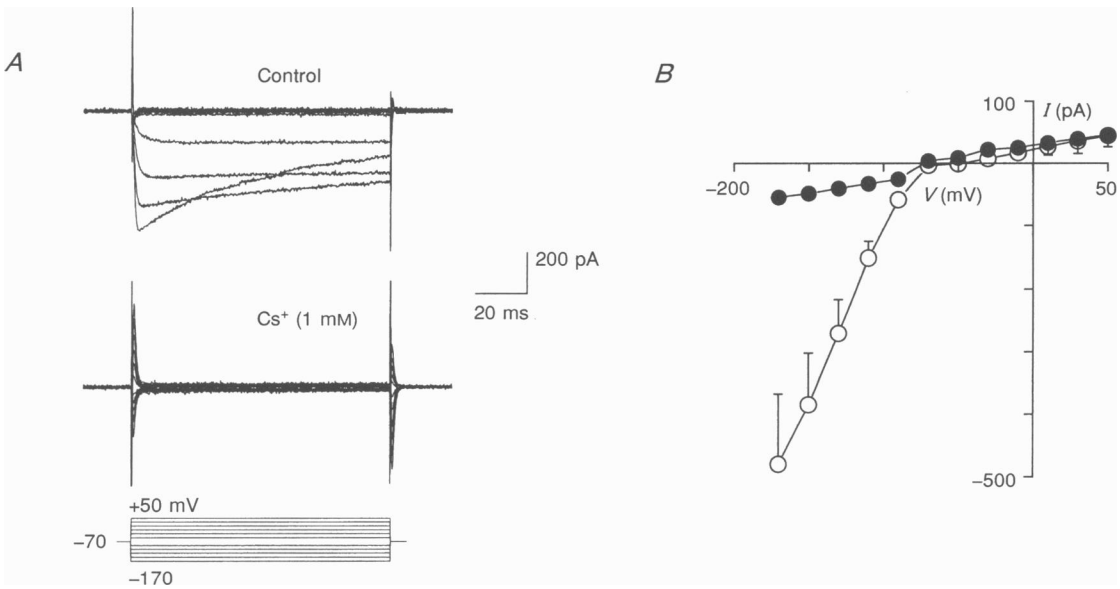

Figure 13. Voltage-dependent inward currents of proliferating rat microglia
A, two families of current amplitudes elicited in the same cell before and after addition of Cs^+ (1 mM) to the bath medium. Currents were evoked by 100 ms voltage pulses every 8 s from a holding potential of −70 mV. Pulse range was from −170 to +50 mV in 20 mV increments. *B*, $I-V$ relations obtained before (○) and after (●) superfusion with a bath solution containing Cs^+ (1 mM). Same protocol as in *A*. Means ± S.E.M. from 6 cells.

Table 2. Effects of potassium channel blockers and Cd^{2+} on the amplitude of voltage-sensitive inward potassium currents in proliferating rat microglia

Treatment	Concentration	Number of experiments	Inhibition of inward current (%)
Cs^+	1 mM	6	83·5 ± 5·0**
Ba^{2+}	5 mM	5	80·5 ± 7·5**
Cd^{2+}	1 mM	4	20·6 ± 8·0
4-Aminopyridine	1 mM	5	22·9 ± 8·6
Tetraethylammonium	10 mM	4	75·2 ± 10·1**

Currents of cultured microglial cells were elicited from a holding potential of −70 mV by both negative and positive voltage pulses of 100 ms duration given in steps of 20 mV. Stimulation was every 8 s. After determining an $I-V$ relation, which demonstrated hyperpolarization-evoked inward currents but no depolarization-evoked outward currents, all compounds and ions were added for 4–8 min to the bath, except tetraethylammonium, which was bath applied for 10–15 min. Then a new $I-V$ relationship was determined in the presence of these compounds. Only one current amplitude was chosen for further evaluation, namely that evoked by a step to −170 mV. The percentage inhibition of this amplitude by the compounds and ions tested was calculated. Statistically significant differences are indicated: *$P < 0.05$; **$P < 0.01$.

Cs^+ (1 mM) and Ba^{2+} (5 mM) (Fig. 13; Table 2). Cd^{2+} (1 mM) and 4-aminopyridine (1 mM) had no effect, while tetraethlyl-ammonium (10 mM) caused a marked inhibition (Table 2).

DISCUSSION

Consequences of a negative slope region in the $I-V$ curve

The membrane potential of microglial cells showed two prominent peaks at −35 and −70 mV. Single cells switched their membrane potential between these preferred values. The $I-V$ curves displayed a characteristic N-like shape with a negative resistance region. A similar non-linear $I-V$ relation containing a region of unstable voltages and resulting in two alternative membrane potential states was reported for mouse peritoneal (Gallin & Livengood, 1981) and spleen macrophages (Gallin, 1981). This characteristic feature of the $I-V$ curve disappeared in macrophages after blockade of inwardly rectifying K^+ channels by Ba^{2+} or Rb^+ (Gallin, 1981; Gallin & Livengood, 1981). Blockers of other types of K^+ conductance, such as 4-aminopyridine and tetraethylammonium, had no effect. The $I-V$ curve of human T-lymphocytes also contained a negative resistance region (Maltsev, 1993). It was suggested that the presence or absence of such a region depends on the ratio of selective K^+ conductance to non-selective leak conductance. We did not try to clarify the reasons for the N-shaped $I-V$ relationship in rat microglial cells.

In proliferating microglial cells (Kettenmann, Banati & Walz, 1993) the membrane potential showed a similarly large variability as in macrophages (Gallin, 1981; Gallin & Livengood, 1981) and T-lymphocytes (Maltsev, 1993). It was hypothesized, however, that in microglial cells with negligible leakage currents the genuine membrane potential is in the range of −70 to −80 mV; lower values were ascribed to a poor quality of the seal (Kettenmann *et al.* 1993). In contrast, we found in both proliferating and LPS-treated microglial cells two prominent peaks in the distribution of the membrane potential, without any indication for a poor quality of the seal. Hence, $I-V$ curves of proliferating microglial cells may also exhibit a negative slope region which does not disappear after activation by LPS.

K^+ selectivity of the inwardly and outwardly rectifying channels

The present study confirms previous work with respect to the presence of inwardly rectifying K^+ channels both in proliferating (Kettenmann *et al.* 1990; Korotzer & Cotman, 1992; Kettenmann *et al.* 1993) and LPS-treated microglia (Nörenberg *et al.* 1992). An increase in the K^+ concentration of the medium from 4·5 to 50 mM shifted the reversal potential of the inward current to more positive values (Kettenmann *et al.* 1990; orenberg *et al.* 1992). Now we determined the $I-V$ curve of LPS-treated microglia both in asymmetric (4·5 mM extracellular) and symmetric (150 mM extracellular) $[K^+]$. As expected for a K^+-selective conductance, in symmetric $[K^+]$ the slope conductance of the inward current increased and the current reversed at around 0 mV.

LPS-treatment of microglia for more than 3 h leads to the appearance of previously rarely occurring outwardly rectifying potassium channels (Nörenberg *et al.* 1992). It was suggested that synthesis of new channel protein takes place, since the protein-synthesis inhibitor cycloheximide co-applied with LPS prevented the appearance of the voltage-dependent outward current. The K^+ selectivity of the outward current was confirmed by the reversal of tail current amplitudes near the calculated K^+ equilibrium potential.

Characteristics of the inwardly rectifying current

The inwardly rectifying conductance of LPS-treated microglia activated at potentials negative to −70 mV, showed half-maximal activation around the potassium equilibrium potential of −90 mV and maximal activation at approximately −120 mV. Currents evoked by voltage steps to potentials more negative than −100 mV inactivated with a fast time course at a normal extracellular K^+ concentration of 4·5 mM. The inactivation followed first-order kinetics and had a rate that increased with membrane hyperpolarization. Both the threshold of activation (compare Figs 2 and 13) and the time course of decay were similar in proliferating and LPS-treated microglia (see also Kettenmann *et al.* 1990). In symmetric $[K^+]$, the time-dependent inactivation almost disappeared. Similar inwardly rectifying K^+ channels have been described in a wide variety of excitable cells (Kolb, 1990). In view of the monocyte origin of microglia it is of particular interest that human blood macrophages (Gallin & McKinney, 1988), murine peritoneal macrophages (Randriamampita & Trautmann, 1987) and the murine macrophage-like cell line J774·1 (Gallin & Sheehy, 1985; Randriamampita & Trautmann, 1987; McKinney & Gallin, 1988) also possess an inwardly rectifying K^+ conductance, which inactivates during voltage steps to potentials more negative than −100 mV. The time constants of decay were similar to those found in microglia (Gallin & Sheehy, 1985; Randriamampita & Trautmann, 1987).

Inactivation of inward currents in both proliferating and LPS-treated microglial cells was absent in a low-Na^+ medium (5 mM). It is noteworthy that when the extracellular $[K^+]$ was increased from 4·5 to 150 mM, NaCl was substituted with an equimolar concentration of KCl and thereby decreased to 10 mM. Hence the small extent of inactivation in symmetric K^+ concentration may be due both to an increased K^+ and a decreased Na^+ concentration in the bath medium. Na^+-dependent inactivation of inwardly rectifying K^+ channels has been described in skeletal muscle (Standen & Stanfield, 1979) and tunicate egg cells (Ohmori, 1978). In those preparations extracellular Na^+ has been shown to block K^+ permeability in a voltage-dependent manner, probably by binding to a site within the membrane. The reversal potential of the $I-V$ curve of microglial cells did not change in low extracellular Na^+, excluding the possibility that the current is carried both by Na^+ and K^+ (I_h; Mayer & Westbrook, 1983). However, some part of the current may be due to a Na^+ activated K^+ conductance (Bader *et al.* 1990), since the amplitudes of inward currents decreased at low $[Na^+]$ (5 mM) and strongly hyperpolarized potentials. Whole-cell patch-clamp measurements cannot resolve the question of whether the Na^+-activated part of the conductance is due to the involvement of a separate population of inwardly rectifying K^+ channels. In contrast to inward currents, outward currents continued to inactivate in a low-Na^+ medium. This may be due to a purely voltage-dependent process of inactivation.

Extracellular Ba^+ (5 mM) and Cs^+ (1 mM), two classic blockers of inwardly rectifying potassium channels (Gay & Stanfield, 1977; Hagiwara, Miyazaki, Moody & Patlak, 1978) nearly abolished the inward currents of both proliferating and LPS-treated microglial cells, while Cd^{2+} and 4-aminopyridine were inactive. This is in accordance with findings in macrophages (Gallin & Sheehy, 1985; Gallin & McKinney, 1988; McKinney & Gallin, 1988). Moreover, inward K^+ currents of proliferating and LPS-treated microglial cells exhibited a similar voltage dependence and similar kinetic characteristics. All these results strongly suggest that the inwardly rectifying K^+ channels in the two states of microglial activation are identical.

Characteristics of the outwardly rectifying K^+ current

The outward conductance activated at potentials positive to −50 mV, showed half-maximal activation at −25 mV and maximal activation at approximately +10 mV. It activated and inactivated during voltage steps much more slowly than the inward conductance. Activation followed a sigmoidal time course while inactivation could be described by a single exponential. The outward current showed steady-state inactivation as well as a marked inactivation upon the second pulse during repetitive depolarizations at 1 Hz. The characteristics of this current were similar to those of the delayed outwardly rectifying K^+ conductance (K_o^+ Gallin, 1991) of human blood macrophages (Nelson, Jow & Jow, 1990), human alveolar macrophages (Nelson, Jow & Popovich, 1990), murine peritoneal macrophages (Ypey & Clapham, 1984) and the murine macrophage-like cell line J774·1 (Gallin & Sheehy, 1985). An outwardly rectifying K^+ conductance of T- and B-lymphocytes (K_n^+; Gardner, 1990) also resembled both K_o^+ and the microglial conductance (Fukushima, Hagiwara & Henkart, 1984; Cahalan, Chandy, Decoursey & Gupta, 1985; Dupuis, Heroux & Payet, 1989).

However, in other respects the outward conductance of microglial cells showed lymphocyte traits. It recovered with two different time constants from inactivation, as demonstrated with a paired pulse protocol (Cahalan *et al.* 1985). This indicates that the K^+ channel may exist in more than one inactivated state. An increase in the concentration of extracellular Ca^{2+} shifted the $I-V$ relation in the positive direction along the voltage axis, without any change in the peak current at +30 mV (Fukushima *et al.* 1984). In contrast, an elevation of the intracellular Ca^{2+} concentration by altering the buffering capacity of the pipette solution markedly inhibited the current at all command potentials. When the ionophore A23187 was used to promote the entry of Ca^{2+} into microglial cells, outward currents decreased. A similar inhibitory effect of high intracellular free Ca^{2+} was observed in T- and B-lymphocytes (Bregestovski, Redkozubov & Alexeev, 1986; Choquet, Sarthou, Primi, Cazenave & Korn, 1987; Dupuis *et al.* 1989; Pahapill & Schlichter, 1992). Ca^{2+} ions were suggested to block the K_n^+ current by binding to a site within the K^+ channel (Grissmer & Cahalan, 1989). It is noteworthy that

the inactivating outward current of macrophages (K_o^+) is not sensitive to Ca^{2+}. There is, however, an outward current, which is activated both by intracellular Ca^{2+} and voltage (Randriamampita & Trautmann, 1987; Gallin & McKinney, 1988; Gallin, 1991).

The microglial outward current resembles in its pharmacological sensitivity both the lymphocyte K_n and the macrophage K_o^+ conductance (Gardner, 1990; Gallin, 1991). Tetraethylammonium and 4-aminopyridine, two classic blockers of the delayed rectifying and transient outward K^+ currents of excitable tissues (Kolb, 1990) inhibited the outward current of microglia. Intracellular Cs^+ abolished the microglial outward current, but decreased the inward current at only largely hyperpolarized membrane potentials. Blockers of voltage-dependent Ca^{2+} channels (Cd^{2+}) and Ca^{2+}-dependent K^+ channels (charybdotoxin, quinine) in excitable tissues (Cook & Quast, 1989), also depressed the outward current. Tetraethylammonium blocked the inward and outward K^+ conductance to a similar extent; quinine had a moderate, while Cd^{2+}, 4-aminopyridine and charybdotoxin had a high selectivity for the outward K^+ conductance. Since in microglia there was no evidence for the existence of voltage-dependent Ca^{2+} channels, Cd^{2+} was supposed to block directly K^+ channels probably by being trapped within the channel. A similar inhibition of the K_n^+ current in lymphocytes by Ca^{2+}-antagonistic divalent cations was reported previously (Matteson & Deutsch, 1984; Dupuis *et al.* 1989; Grissmer & Cahalan, 1989). Charybdotoxin (Sands, Lewis & Cahalan, 1989) and quinine (Fukushima *et al.* 1984) also block K_n^+ channels of lymphocytes (Gardner, 1990). Finally, the presence of a recently cloned lymphocyte K_n^+ channel (RGK5; Douglass, Osbourne, Cai, Wilkinson, Christie & Adelman, 1990) has been proven in rat microglia using molecular biology methods (Nörenberg, Appel, Bauer, Gebicke-Haerter & Illes, 1993).

Physiological role of the outwardly rectifying K^+ current

The inwardly rectifying K^+ channels are setting the membrane potential to its resting level after hyperpolarizing stimuli (Gallin, 1991). However, these K^+ channels of microglial cells can only marginally counteract depolarizations (Kettenmann *et al.* 1993). Such depolarizations may be due in macrophages to the binding of immunoglobulin G (IgG) to Fc-receptors (Young, Unkeless, Young, Mauro & Cohn, 1983) or ATP to P_2-purinoceptors (Sung, Young, Origlio, Heiple, Kaback & Silverstein, 1985) and the subsequent opening of non-selective cationic channels. Recently, ATP has been shown to cause a long-lasting depolarization in proliferating microglia (Kettenmann *et al.* 1993) which is considerably shorter in LPS-activated microglia (Nörenberg, Langosch, Gebicke-Haerter & Illes, 1994). Various inflammatory stimuli such as LPS and interferon-γ lead to the expression of outwardly rectifying K^+ channels in microglia (Nörenberg *et al.* 1992). During inflammation or cellular damage, the IgG and ATP levels in the extracellular space may increase. Hence, there is a higher likelihood that differentiated (macrophage-like) microglia are depolarized by these stimuli than proliferating microglia; the development of efficient means to counteract this depolarization may be a necessary adaptive mechanism.

The mixed macrophage–lymphocyte characteristics of the outward K^+ conductance of microglial cells appear to be a special feature of this cell type. Since lymphocytes are almost absent in the central nervous system, but have important roles in immune responses to inflammatory stimuli, monocyte-derived microglia may have acquired some lymphocyte properties.

REFERENCES

Adams, D. O. & Hamilton, T. A. (1987). Molecular transductional mechanisms by which IFNγ and other signals regulate macrophage development. *Immunological Reviews* **97**, 5–27.

Bader, C. R., Bernheim, L., Bertrand, D. & Haimann, C. (1990). Sodium-activated potassium currents. In *Potassium Channels. Structure, Classification, Function and Therapeutic Potential*, ed. Cook, N. S., pp. 155–166. Ellis Horwood, Chichester, UK.

Banati, R. B., Hoppe, D., Gottmann, K., Kreutzberg, G. W. & Kettenmann, H. (1991). A subpopulation of bone marrow-derived macrophage-like cells shares a unique ion channel pattern with microglia. *Journal of Neuroscience Research* **30**, 593–600.

Bignami, A. (1991). Glial cells in the central nervous system. *Discussions in Neuroscience* **8**, 11–45.

Bregestovski, P., Redkozubov, A. & Alexeev, A. (1986). Elevation of intracellular calcium reduces voltage-dependent potassium conductance in human T cells. *Nature* **319**, 776–778.

Cahalan, M. D., Chandy, K. G., Decoursey, T. E. & Gupta, S. (1985). A voltage-gated potassium channel in human T lymphocytes. *Journal of Physiology* **358**, 197–237.

Choquet, D., Sarthou, P., Primi, D., Cazenave, P.-A. & Korn, H. (1987). Cyclic AMP-modulated potassium channels in murine B cells and their precursors. *Science* **235**, 1211–1214.

Cook, N. S. & Quast, U. (1989). Potassium channel pharmacology. In *Potassium Channels. Structure, Classification, Function and Therapeutic Potential*, ed. Cook, N. S., pp. 181–255. Ellis Horwood, Chichester, UK.

Dickson, D. W., Mattiace, L. A., Kure, K., Hutchins, K., Lyman, W. D. & Brosnan, C. F. (1991). Biology of disease. Microglia in human disease, with an emphasis on acquired immune deficiency syndrome. *Laboratory Investigations* **64**, 135–156.

Dijkstra, C. D., Döpp, E. A., Joling, P. & Kraal, G. (1985). The heterogeneity of mononuclear phagocytes in lymphoid organs: distinct macrophage subpopulations in the rat recognized by monoclonal antibodies ED1, ED2 and ED3. *Immunology* **54**, 589–599.

Douglass, J., Osborne, P. B., Cai, Y.-C., Wilkinson, M., Christie, M. J. & Adelman, J. P. (1990). Characterization and functional expression of a rat genomic DNA clone encoding a lymphocyte potassium channel. *Journal of Immunology* **144**, 4841–4850.

Dupuis, G., Heroux, J. & Payet, M. D. (1989). Characterization of Ca^{2+} and K^+ currents in the human Jurkat T cell line: effects of phytohaemagglutinin. *Journal of Physiology* **412**, 135–154.

Fukushima, Y., Hagiwara, S. & Henkart, M. (1984). Potassium current in clonal cytotoxic T lymphocytes from the mouse. *Journal of Physiology* **351**, 645–656.

Galanos, C., Lüderitz, O. & Westphal, O. (1979). Preparation and properties of a standardized lipopolysaccharide from Salmonella abortus equi (Novo-Pyrexal). *Zentralblatt für Bakteriologie und Hygiene* **243**, 226–244.

Gallin, E. K. (1981). Voltage clamp studies in macrophages from mouse spleen cultures. *Science* **214**, 458–460.

GALLIN, E. K. (1991). Ion channels in leukocytes. *Physiological Reviews* **71**, 775–811.

GALLIN, E. K. & LIVENGOOD, D. R. (1981). Inward rectification in mouse macrophages: evidence for a negative resistance region. *American Journal of Physiology* **241**, C9–17.

GALLIN, E. K. & MCKINNEY, L. C. (1988). Patch-clamp studies in human macrophages: single channel and whole-cell characterization of two K^+ conductances. *Journal of Membrane Biology* **103**, 55–66.

GALLIN, E. K. & SHEEHY, P. A. (1985). Differential expression of inward and outward potassium currents in the macrophage-like cell line J774·1. *Journal of Physiology* **369**, 475–499.

GANTER, S., NORTHOFF, H., MÄNNEL, D. & GEBICKE-HAERTER, P. J. (1992). Growth control of cultured microglia. *Journal of Neuroscience Research* **33**, 218–230.

GARDNER, P. (1990). Potassium channels in immunoresponsive cells. In *Potassium Channels. Structure, Classification, Function and Therapeutic Potential*, ed. COOK, N. S., pp. 382–399. Ellis Horwood, Chichester, UK.

GAY, L. A. & STANFIELD, P. R. (1977). Cs^+ causes a voltage-dependent block of inward K currents in resting skeletal muscle fibres. *Nature* **267**, 169–170.

GEBICKE-HAERTER, P. J., BAUER, J., SCHOBERT, A. & NORTHOFF, H. (1989). Lipopolysaccharide-free conditions in primary astrocyte cultures allow growth and isolation of microglial cells. *Journal of Neuroscience* **9**, 183–194.

GRISSMER, S. & CAHALAN, M. D. (1989). Divalent ion trapping inside potassium channels of human T lymphocytes. *Journal of General Physiology* **93**, 609–630.

HAGIWARA, S., MIYAZAKI, S., MOODY, W. & PATLAK, J. (1978). Blocking effect of barium and hydrogen ions on the potassium current during anomalous rectification in the starfish egg. *Journal of Physiology* **279**, 167–185.

HAMILL, O. P., MARTY, E., NEHER, E., SAKMANN, B. & SIGWORTH, F. J. (1981). Improved patch-clamp techniques for high-resolution current recording from cells and cell-free membrane patches. *Pflügers Archiv* **391**, 85–100.

HAMILTON, T. A. & ADAMS, D. O. (1987). Molecular mechanisms of signal transduction in macrophages. *Immunology Today* **8**, 151–158.

HODGKIN, A. L. & HUXLEY, A. F. (1952). A quantitative description of membrane current and its application to conduction and excitation in nerve. *Journal of Physiology* **117**, 500–544.

HORN, R. & MARTY, A. (1988). Muscarinic activation of ionic currents measured by a new whole-cell recording method. *Journal of General Physiology* **92**, 145–159.

JORDAN, F. L. & THOMAS, W. E. (1988). Brain macrophages: questions of origin and interrelationship. *Brain Research Reviews* **13**, 165–178.

KELLER, M., JACKISCH, R., SEREGI, A. & HERTTING, G. (1985). Comparison of prostanoid forming capacity of neuronal and astroglial cells in primary cultures. *Neurochemistry International* **7**, 655–665.

KETTENMANN, H., BANATI, R. & WALZ, W. (1993). Electrophysiological behavior of microglia. *Glia* **7**, 93–101.

KETTENMANN, H., HOPPE, D., GOTTMANN, K., BANATI, R. & KREUTZBERG, G. (1990). Cultured microglial cells have a distinct pattern of membrane channels different from peritoneal macrophages. *Journal of Neuroscience Research* **26**, 278–287.

KOLB, H.-A. (1990). Potassium channels in excitable and non-excitable cells. *Reviews of Physiology, Pharmacology and Biochemistry* **115**, 51–91.

KOROTZER, A. R. & COTMAN, C. W. (1992). Voltage-gated currents expressed by rat microglia in culture. *Glia* **6**, 81–88.

MCKINNEY, L. C. & GALLIN, E. K. (1988). Inwardly rectifying whole cell and single-channel K currents in the murine macrophage cell line J774·1. *Journal of Membrane Biology* **103**, 41–53.

MCKINNEY, L. C. & GALLIN, E. K. (1990). Effect of adherence, cell morphology, and lipopolysaccharide on potassium conductance and passive membrane properties of murine pacrophage J774·1 cells. *Journal of Membrane Biology* **116**, 47–56.

MALTSEV V. A. (1993). A negative resistance region underlies the triggering property of membrane potential of human T-lymphocytes. *Cellular Signalling* **4**, 697–707

MATTESON, D. R. & DEUTSCH, C. (1984). K channels in T lymphocytes: a patch clamp study using monoclonal antibody adhesion. *Nature* **307**, 468–471.

MAYER, M. L. & WESTBROOK, G. L. (1983). A voltage-clamp analysis of inward (anomalous) rectification in mouse spinal sensory ganglion neurones. *Journal of Physiology* **340**, 19–45.

NELSON, D. J., JOW, B. & JOW, F. (1990). Whole-cell currents in macrophages: I. Human monocyte-derived macrophages. *Journal of Membrane Biology* **117**, 29–44.

NELSON, D. J., JOW, B. & JOW, F. (1992). Lipopolysaccharide induction of outward potassium current expression in human monocyte-derived macrophages: lack of correlation with secretion. *Journal of Membrane Biology* **125**, 207–218.

NELSON, D. J., JOW, B. & POPOVICH, K. J. (1990). Whole-cell currents in macrophages: II. Alveolar macrophages. *Journal of Membrane Biology* **117**, 45–55.

NORTHOFF, H., GLÜCK, A., WÖLPL, B., KUBANEK, B. & GALANOS, C. (1986). Lipopolysaccharide-induced elaboration of interleukin-1 (IL-1) by human monocytes: use for the detection of LPS in serum and influence of serum-LPS interaction. *Reviews of Infectious Diseases* **9**, suppl. 5, 599–602.

NÖRENBERG, W., APPEL, K., BAUER, J., GEBICKE-HAERTER, P. J. & ILLES, P. (1993). Expression of an outwardly rectifying K^+ channel in rat microglia cultivated on teflon. *Neuroscience Letters* **160**, 69–72.

NÖRENBERG, W., GEBICKE-HAERTER, P. J. & ILLES, P. (1992). Inflammatory stimuli induce a new K^+ outward current in cultured rat microglia. *Neuroscience Letters* **147**, 171–174.

NÖRENBERG, W., LANGOSCH, J. M., GEBICKE-HAERTER, P. J. & ILLES, P. (1994). Characterization and possible function of adenosine 5′-triphosphatereceptors in activated rat microglia. *British Journal of Pharmacology* (in the Press).

NOVIKOFF, A. B. & GOLDFISCHER, S. (1961). Nucleoside-diphosphatase activity in the Golgi apparatus and its usefulness for cytological studies. *Proceedings of the National Academy of Sciences of the USA* **47**, 802–810.

OHMORI, H. (1978). Inactivation kinetics and steady-state current noise in the anomalous rectifier of tunicate egg cell membranes. *Journal of Physiology* **281**, 77–99.

PAHAPILL, P. A. & SCHLICHTER, L. C. (1992). Modulation of potassium channels in intact human T lymphocytes. *Journal of Physiology* **445**, 407–430.

RANDRIAMAMPITA, C. & TRAUTMANN, A. (1987). Ionic channels in murine macrophages. *Journal of Cell Biology* **105**, 761–769.

RIESKE, E., GRAEBER, M. B., TETZLAFF, W., CZLONKOWSKA, A., STREIT, W. J. & KREUTZBERG, G. W. (1989). Microglia and microglia-derived brain macrophages in culture: generation from axotomized rat facial nuclei, identification and characterization *in vitro*. *Brain Research* **492**, 1–14.

SANDS, S. B., LEWIS, R. S. & CAHALAN, M. D. (1989). Charybdotoxin blocks voltage-gated K^+ channels on human and murine T lymphocytes. *Journal of General Physiology* **93**, 1061–1074.

STANDEN, N. B. & STANFIELD, P. R. (1979). Potassium depletion and sodium block of potassium currents under hyperpolarization in frog sartorius muscle. *Journal of Physiology* **294**, 497–520.

STREIT, W. J. (1990). An improved staining method for rat microglial cells using the lectin from *Griffonia simplicifolia* (GSA I-B4). *Journal of Histochemistry and Cytochemistry* **38**, 1683–1686.

STREIT, W. J., GRAEBER, M. B. & KREUTZBERG, G. W. (1988). Functional plasticity of microglia: a review. *Glia* **1**, 301–307.

Sung, S. S.-J., Young, J. D.-E., Origlio, A. M., Heiple, J. M., Kaback, H. R. & Silverstein, S. C. (1985). Extracellular ATP perturbs transmembrane ion fluxes, elevates cytosolic [Ca^{2+}], and inhibits phagocytosis in mouse macrophages. *Journal of Biological Chemistry* **260**, 13442–13449.

Theele, D. P. & Streit, W. J. (1993). A chronicle of microglial ontogeny. *Glia* **7**, 5–8.

Thomas, W. E. (1992). Brain macrophages: evaluation of microglia and their funtions. *Brain Research Reviews* **17**, 61–74.

Young, J. D.-E., Unkeless, J. C., Young, T. M., Mauro, A. & Cohn, Z. A. (1983). Role for mouse macrophage IgG Fc receptor as ligand-dependent ion channel. *Nature* **306**, 186–189.

Ypey, D. L. & Clapham, D. E. (1984). Development of a delayed outward-rectifying K^+ conductance in cultured mouse peritoneal macrophages. *Proceedings of the National Academy of Sciences of the USA* **81**, 3083–3087.

Acknowledgements

We are grateful to Mr J. Langosch for valuable help with some of the experiments and to Drs R. Greger and K. Haverkampf for critically reading the manuscript. This work was supported by grants of the Deutsche Forschungsgemeinschaft to P.I. (SFB 325, A2) and P.J.G.-H. (Schwerpunkt Glia, Ge 486/6–1).

Received 15 April 1993; accepted 29 July 1993.